INVERSE ČERENKOV ACCELERATOR RESULTS

W. D. Kimura, STI Optronics, Inc., 2755 Northup Way, Bellevue, WA 98004 USA

Laser acceleration experiments of relativistic electrons utilizing the inverse Čerenkov effect, whereby a gas slows the phase velocity of the laser light to match the electron velocity, have recently demonstrated >30 MeV/m acceleration gradients over a 12-cm interaction length using a ~580-MW CO_2 laser beam. These experiments were performed at the Brookhaven National Laboratory Accelerator Test Facility (ATF). With a 5-GW laser pulse, an energy gain of >12 MeV is predicted over a 20-cm interaction length corresponding to >60 MeV/m acceleration gradient. Future experiments will examine prebunching the electrons to optical wavelengths and staging the acceleration process. The CO_2 laser is also being upgraded to produce higher peak power. With 250-GW peak power, the goal is to eventually demonstrate 100 MeV net energy gain and an acceleration gradient of >300 MeV/m.

I. INTRODUCTION

Using lasers to accelerate relativistic particles offers the potential for generating >1 GeV/m acceleration gradients. These high gradients are necessary for the next generation of TeV-class (10^{12} eV) electron accelerators needed for high energy physics research. Such high gradients would also make it possible to construct compact accelerators for use in industry and medicine.

The inverse Čerenkov effect was first demonstrated at Stanford University in 1981 [1]. Fontana and Pantell [2] later developed an improved configuration for inverse Čerenkov acceleration (ICA). Their basic scheme is shown in Fig. 1, which is taken from Ref. 2. A radially polarized laser beam is focused by an axicon onto the *e*-beam traveling through a gas-filled interaction region. The light intersects the *e*-beam at the Čerenkov angle θ_C, where $\theta_C = \cos^{-1}(1/n\beta)$, n is the index of refraction of the gas and β is the ratio of the electron velocity to the speed of light.

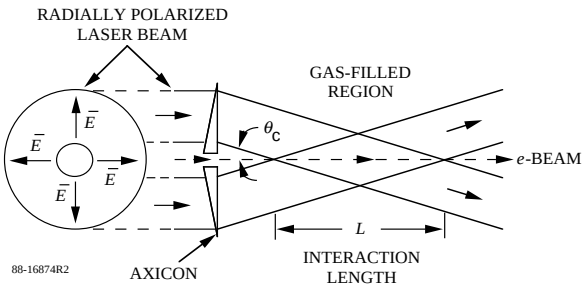

Figure 1: Inverse Čerenkov acceleration configuration [2]. A radially polarized laser beam is focused by an axicon onto the *e*-beam at the Čerenkov angle θ_C inside a gas-filled region, resulting in energy exchange occurring over an interaction length *L*.

The basic Fontana/Pantell geometry is the one used in the present and planned ICA experiments. This configuration has important advantages over the geometry used during the Stanford experiments. It produces a more efficient coupling of the laser energy into the *e*-beam and the *e*-beam can be focused axisymmetrically. This helps to mitigate some of the detrimental effects of gas scattering by channeling the electrons in the longitudinal direction [3]. This same effect also allows using the inverse Čerenkov effect as a beam focuser.

II. DESCRIPTION OF EXPERIMENT

The experiment [4] is performed on the Accelerator Test Facility (ATF) located at Brookhaven National Laboratory (BNL). This facility features a 40-MeV electron accelerator that uses a photocathode microwave electron gun driven by a Nd:YAG (4ω) laser. This same laser is used to switch out short pulses from a linearly-polarized CO_2 laser (λ = 10.6 μm) utilizing semiconductor switching. These short pulses are then amplified and are available for laser particle acceleration experiments [5]. Table 1 lists the characteristics of the ATF linac and laser system. (Note that the ATF *e*-beam emittance has been substantially improved since the ICA experiment and is now ~1 π mm-mrad.)

The major components of the experiment are a gas cell where the ICA interaction occurs, an optical system for converting the linearly-polarized ATF CO_2 laser beam into one with radial polarization [6], and an electron beam transport line and diagnostic devices connected to the gas cell.

Figure 2 is a schematic plan view of the gas cell showing the 45° mirror used to direct the incoming laser beam towards the axicon mirror that focuses the laser beam onto

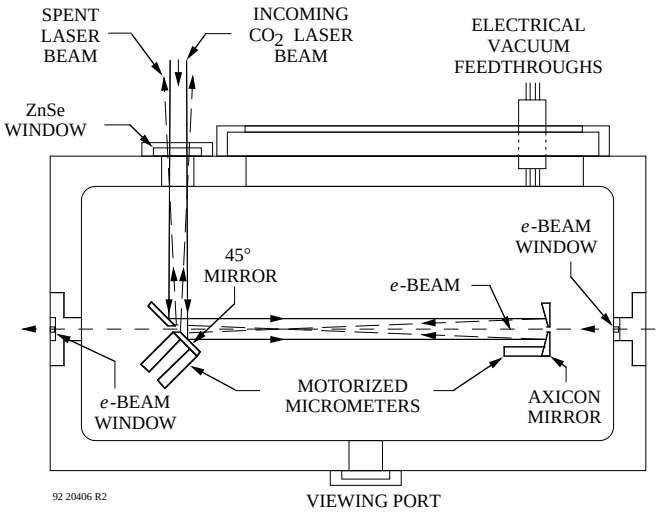

Figure 2: Schematic plan view of gas cell.

the *e*-beam traveling from right to left in the figure. An axicon mirror is used rather than a lens as depicted in Fig. 1 because of the higher laser damage threshold of metal mirrors. The axicon mirror is remotely adjustable. Table 1 lists the other parameters for the gas cell. Note that θ_C = 20 mrad and that the interaction length is 12 cm.

TABLE 1. ICA Experiment System Parameters

Electron Beam	
Source:	BNL ATF
Beam energy:	40 MeV
Intrinsic energy spread (σ):	≈±0.5 MeV
Normalized emittance:	~20 π mm-mrad
Electron bunch length:	≈10 ps (FWHM)
Charge per bunch:	≈0.1 nC
Pulse format:	Single pulse
Laser Beam	
Laser:	CO_2
Wavelength:	10.6 μm
Pulse length:	220 ps
Peak power delivered to interaction region:	~580 MW
Pulse repetition rate:	Single shot
Interaction Region (Gas Cell)	
Phase matching medium:	Hydrogen gas
Čerenkov angle:	20.08 mrad ± 0.08 mrad
Temperature:	16.7 °C
Length of electron/laser beam overlap:	≈12 cm
Length of gas traversed by electrons:	43 cm
Thickness of diamond film *e*-beam windows:	2.1 μm

The ATF CO_2 laser is capable of generating ~10 GW of peak output power. However, the amount of peak power that could be delivered to the interaction was limited by one of the optical elements in the ICA optical system. Although this situation was rectified after the experiment, it meant during the experiment the effective peak power delivered to the interaction region was ~580 MW. This effective power includes a correction factor because the delivered laser beam was also only 83% radially polarized. (Normally this is >90%.)

III. EXPERIMENTAL RESULTS

The spectrometer has a momentum acceptance range of ±2.8% of the mean energy. Since the ICA interaction resulted in an energy modulation much larger than this range, it was necessary during the experiment to scan the spectrometer and use multiple shots to obtain subspectra in order to construct the full modulated spectrum. The subspectra are corrected for the spectrometer momentum acceptance and dispersion characteristics based upon separate measurements and modeling performed on the spectrometer.

Some pulse-to-pulse changes in the *e*-beam and laser beam characteristics occurred during the scan. The largest fluctuations were in the *e*-beam current ($\sigma \approx 50\%$), which fortunately only changed the magnitude of the spectrometer signal and not the overall shape of the full spectrum. Instabilities of the mean *e*-beam energy due to RF power fluctuations added a ≈±93 keV uncertainty in the energy values of the full spectrum; but, as will be shown, this is much less than the acceleration imparted upon the *e*-beam by the laser. Lastly, the laser pulse energy varied with a $\sigma \approx$ 14%; however, since the ICA interaction scales with the square-root of the laser peak power [2], this amount of variation does not appreciably change the shape of the full spectrum. Thus, even though the conditions are not exactly the same for each of the subspectra, an approximate full spectrum can be created by scaling the subspectra to fit end-to-end to compensate for the variations in *e*-beam current.[1]

To avoid adding more complications during the scanning process, the gain of the spectrometer detector (image intensifier and CCD camera) was kept constant during the scan. However, this also limited the ability to detect faint signals above the noise level of the CCD camera associated with the highest accelerated and decelerated electrons. These electrons were detected in separate measurements by setting the spectrometer detector to maximum gain. These results will be shown in a later figure.

Figure 3 shows the *e*-beam energy spectra results for the experimental conditions listed in Table 1. Figure 3(a) shows the energy spectrum after traversing through the gas cell filled with 2.2 atm of H_2 with the laser off. Most of the energy spread is due to the intrinsic width of the *e*-beam ($\sigma \approx$ 0.5 MeV). Figure 3(b) shows the result with the laser delivering ~580-MW of peak power to the interaction region, where the subspectra have been spliced together to yield an approximate full spectrum. Since the electron bunch length (τ/c ~ 4 mm) is much longer than the laser wavelength, the interaction between the *e*-beam and the laser beam occurred over all phases of the laser light wave, resulting in both accelerated and decelerated electrons being observed.

The subspectra obtained at the highest spectrometer detector gain is given in Fig. 4. Electrons at ~3.7 MeV are observed corresponding to an acceleration gradient of ≈31 MeV/m over the 12-cm interaction length. Our model [3] predicted a peak acceleration gradient of 35 MeV/m, which is consistent with the measurements. Note that only a relatively small number of electrons gain high energy. This can be significantly increased by prebunching the electrons before they interact with the laser beam such that the

[1] A Faraday cup was positioned at the output end of the spectrometer for measuring the *e*-beam current; however, it was limited by noise during the experiment. This limitation also prevented using this current sensor for monitoring fluctuations in the *e*-beam current.

electron bunch intersects the light wave at the phase point for optimum acceleration. Then most of the electrons in the bunch would gain high energy.

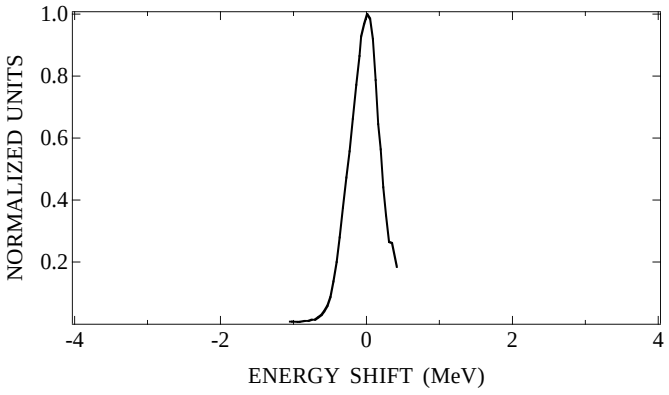

(a)

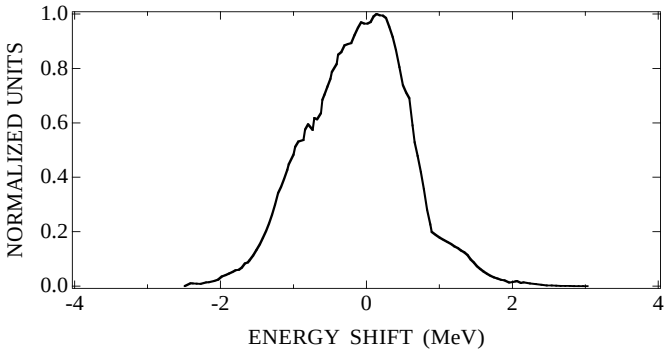

(b)

Figure 3: Electron-beam energy spectra. (a) With no laser present and after traveling through the gas cell filled with 2.2 atm H_2 at 16.7°C. (b) With ~580 MW of laser peak power delivered to the interaction region and measured at constant spectrometer gain (see text).

Current detector limitations (see Footnote 1) prevented the number of electrons accelerated to higher energies from being quantified during this particular experiment. However, a strong spectrometer signal was obtained which indicated that a significant fraction of the total number of electrons in the *e*-beam pulse were being accelerated with each shot. Based upon the sensitivity of the spectrometer detector system, we estimate that the spectrum shown in Fig. 3(b) corresponds to roughly 10 pC of charge. Based on the shape of the model curve we estimate that $>10^6$ electrons received energy gains >2 MeV.

The pressure was varied to optimize the interaction and, based upon the optimum pressure point, to determine the effective Čerenkov angle of the experiment. Figure 5 shows the measured pressure dependence of the ICA process. Plotted is the width of the normalized central subspectrum (at 80% of the peak) versus pressure. Note that the maximum for the data occurs at a gas pressure that corresponds to a Čerenkov angle of ~19.4 mrad. This may be caused by an imperfectly collimated laser beam at the axicon.

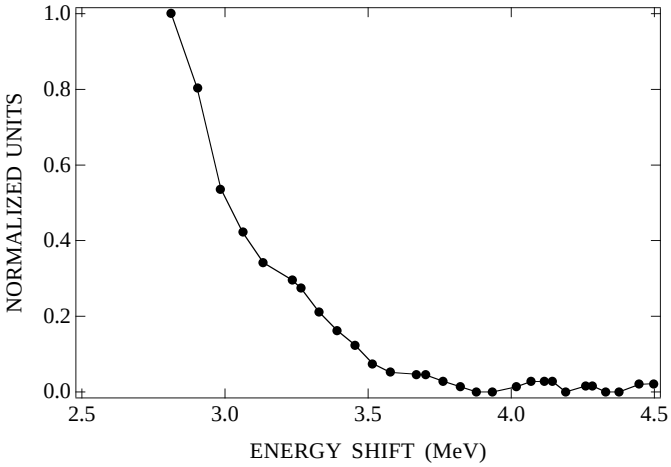

Figure 4: Electron beam energy subspectrum obtained at the highest spectrometer detector gain. The other parameters are the same as in Fig. 3.

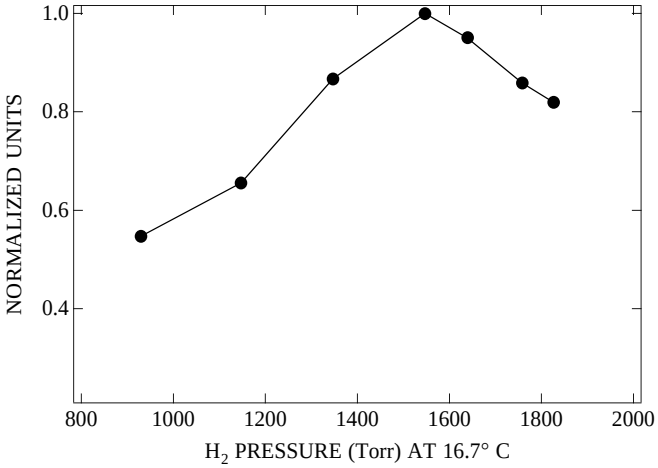

Figure 5: Gas pressure dependence results.

During the next experimental run approximately 5 GW of laser peak power will be delivered to the interaction region and the interaction length will be increased to ~20 cm. Under these conditions the model predicts >12 MeV peak acceleration corresponding to a >60 MeV/m acceleration gradient. The *e*-beam current monitoring capabilities will also be improved.

IV. 100-MeV INVERSE ČERENKOV LASER ACCELERATION EXPERIMENT

The success of the present ICA experiments gives us confidence to improve the process and scale it up to higher energies. We are presently beginning the next phase of the experiments to demonstrate 100 MeV net energy gain using ICA. The goals of the experiment are to: 1) Demonstrate prebunching of the *e*-beam at optical wavelengths. This is

important for efficient acceleration. 2) Demonstrate staging of acceleration sections, where the primary issue is rephasing the light wave with the bunched electrons. Staging is important for scaling to higher energy gains. 3) Compensate for phase slippage within each stage. At high acceleration gradients the electrons gain enough energy that they lose phase matching along the interaction length. Compensation is important for maximizing the net acceleration. And, 4) demonstrate 100 MeV net acceleration of $\geq 5 \times 10^8$ electrons/pulse. While the peak energy gain depends primarily on the laser peak power, the total number of accelerated electrons is affected by many other factors, such as gas scattering, emittance, and trapping efficiency. Hence, reaching the goal of $\geq 5 \times 10^8$ electrons/pulse will require controlling these factors.

Figure 6 shows the conceptual layout for the 100-MeV laser accelerator. The upgraded ATF *e*-beam (65 MeV) is sent into an ICA prebuncher whose output feeds directly into a magnetic chicane (compressor). The magnetic chicane is a device that shortens the distance required to achieve maximum bunching density of the electrons after they exit the prebuncher. Without this device the *e*-beam will diverge too much before optimum bunching has occurred. Hence, the compressor helps keep the overall system short. After the chicane there will be a drift space where magnetic focusing and steering elements refocus the bunched *e*-beam into the ICA accelerator.

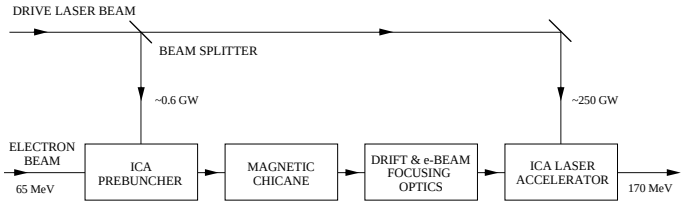

Figure 6: Conceptual layout for the 100-MeV ICA laser accelerator.

The 100-MeV laser accelerator experiment will use most of the existing ICA hardware, including the radial polarization converter system and the present gas cell, which will be modified to act as the prebuncher. The prebuncher will have a much shorter interaction length (~4-5 cm) and roughly 0.6 GW of laser peak power will be used to drive it.

A preliminary design for the experiment is given in Fig. 7. The ICA accelerator will consist of a single-stage, 27-cm long interaction length that is very similar in design to the present gas cell (see Fig. 2). One important difference is that it will use a curved axicon to compensate for phase slippage within the interaction region. Recall that $\theta_c = \cos^{-1}(1/n\beta)$; thus as β increases, θ_c needs to increase in order to maintain the same phase matching condition. This can be achieved by continuously increasing the angle of intersection along the interaction length in a manner analogous to a tapered wiggler. This is depicted in Fig. 8. Note, that for the conditions of our experiment, the actual angle change is very small (~1 mrad).

In order to achieve 100 MeV energy gain, the ATF CO_2 laser needs to deliver ≥250 GW to the ICA accelerator. The ATF has received initial funding to upgrade the laser. Once the upgrade is completed the laser is expected to produce at least several 100 GW output.

Phase synchronization between the prebuncher and the accelerator will be achieved by adjusting the optical delay depicted at the bottom of Fig. 7. Note, that between the prebuncher and the accelerator, the *e*-beam will be traveling through a vacuum tube.

We anticipate that the primary technical issue facing this experiment will be laser damage of optical components. However, we believe the system can be designed to avoid this. Laser-induced gas breakdown should not be an issue based upon calculations using the Keldysh formulas [7].

The experiment will be performed in phases. Phase 1(a) will be occurring after the next experimental run. The objective will be to demonstrate optical prebunching. Tight *e*-beam focusing into the interaction region and minimizing

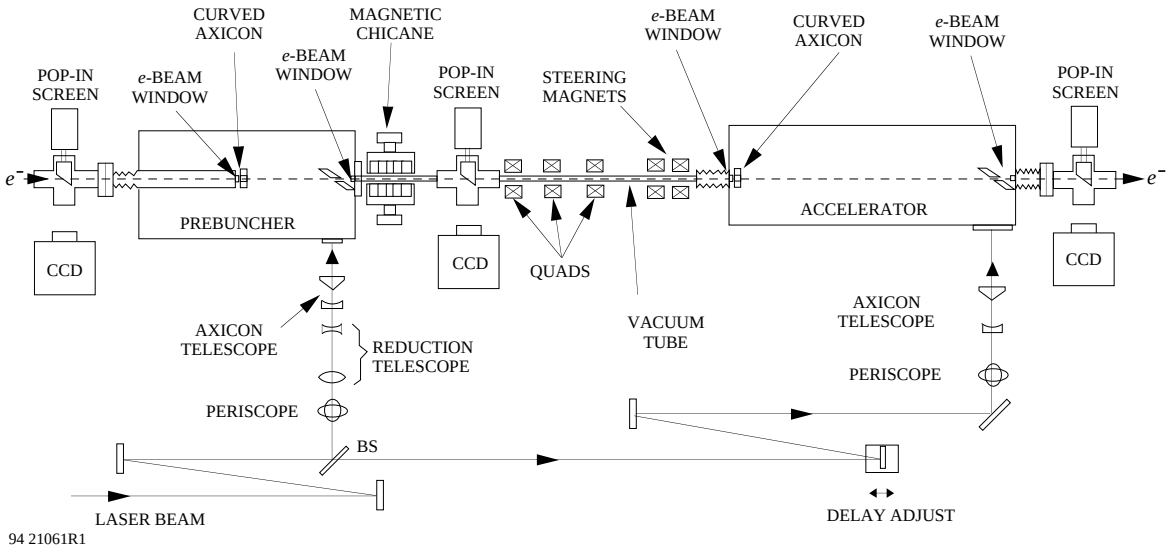

Figure 7: Preliminary design for 100-MeV laser accelerator experiment.

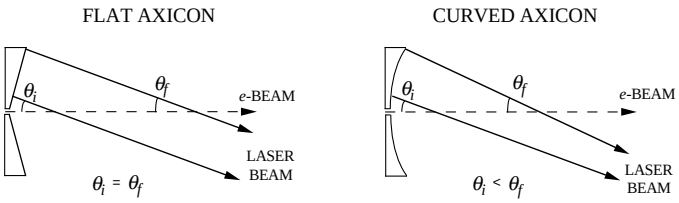

Figure 8: Basic focusing characteristics of flat and curved axicons.

gas scattering will be important. An issue during this phase is determining the best way to measure the bunched *e*-beam characteristics. Examining effects such as enhanced Čerenkov or optical transition radiation are possibilities. Phase 1(b) will incorporate the magnetic chicane and other beamline hardware (e.g., focusing quadrupoles and steering magnets) into the system. We plan to make the chicane using rare-earth permanent magnets and take advantage of the extensive wiggler/undulator design and fabrication experience at STI. Phase 1(c) will add the ICA accelerator to the system and will demonstrate rephasing between the bunched electrons and laser light. To avoid possible laser damage problems, the Phase 1(c) experiments will be performed using the existing 10-GW ATF CO_2 laser beam. Finally, during Phase II the upgraded laser power (≥250 GW) will be delivered to the ICA accelerator for demonstration of 100 MeV energy gain.

The 100-MeV laser accelerator experiment will set the stage for scaling this process to even higher energies by demonstrating important "building block" capabilities, such as prebunching, trapping, staging, and rephasing. The next goal will be to use this knowledge to demonstrate 1 GeV net acceleration. A 100-MeV energy gain over the 27-cm long ICA accelerator corresponds to ~370 MeV/m. Hence, in principle, 1 GeV could be achieved in <4 m. Of course, an actual 1-GeV laser accelerator will be longer than this, but it demonstrates that a 1-GeV ICA system can be reasonable in size. Such a system would probably use multiple ICA stages.

One of the advantages of ICA is that it should be possible to recycle the laser beam to reintersect the *e*-beam and continue the acceleration process. The basic scheme is illustrated in Fig. 9. The cylindrical mirror tube is optically equivalent to the axicon mirror. Recycling the laser pulse helps improve the efficiency of the process.

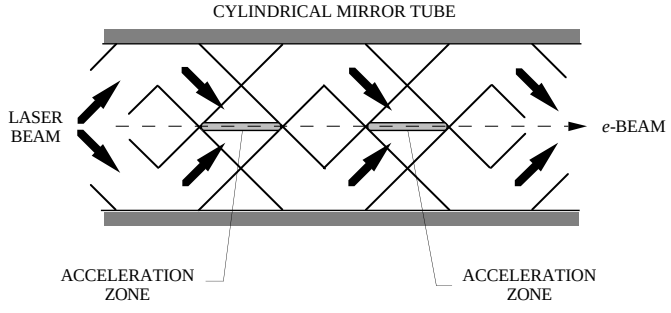

Figure 9: Schematic of possible method for recycling the laser pulse between multiple ICA stages.

V. CONCLUSION

Recent ICA experiments performed on the ATF have demonstrated ≤3.7 MeV acceleration is good agreement with theory. During the next experimental run we anticipate demonstrating >12 MeV energy gain corresponding to an acceleration gradient of >60 MeV/m. Preparations for the 100-MeV ICA laser accelerator experiment on the ATF are underway. The first phase of the experiment will demonstrate prebunching of the *e*-beam at optical wavelengths. This effort will be one of the first in the field of laser acceleration research to demonstrate prebunching and staging. The capabilities demonstrated will directly help in the design of a 1-GeV ICA demonstration experiment.

VI. ACKNOWLEDGMENTS

The author wishes to acknowledge the other collaborators in this research program: G. H. Kim, R. D. Romea, and L. C. Steinhauer at STI Optronics; I. V. Pogorelsky, K. P. Kusche, R. C. Fernow, and X. Wang at BNL; and Y. Liu at the University of California, Los Angeles. This work was supported by the U.S. Department of Energy under Grant No. DE-FG06-93ER40803.

VII. REFERENCES

[1] J. A. Edighoffer, W. D. Kimura, R. H. Pantell, M. A. Piestrup, and D. Y. Wang, "Observation of inverse Čerenkov interaction between free electrons and laser light," Phys. Rev. A **23**, 1848-1854, (1981).

[2] J. R. Fontana and R. H. Pantell, "A high-energy, laser accelerator for electrons using the inverse Cherenkov effect," J. Appl. Phys. **54**, 4285-4288, (1983).

[3] R. D. Romea and W. D. Kimura, "Modeling of inverse Čerenkov laser acceleration with axicon laser beam focusing," Phys. Rev. D **42**, 1807-1818 (1990).

[4] W. D. Kimura, G. H. Kim, R. D. Romea, L. C. Steinhauer, I. V. Pogorelsky, K. P. Kusche, R. C. Fernow, X. Wang, and Y. Liu, "Laser acceleration of relativistic electrons using the inverse Čerenkov effect," Phys. Rev. Lett. **74**, 546-549 (1995).

[5] I. Pogorelsky, "High power picosecond CO_2 laser system for ATF electron accelerator project," in *Advanced Accelerator Concepts*, Port Jefferson, NY, AIP Conference Proceedings No. 279, J. S. Wurtele, Ed., (American Institute of Physics, New York, 1993), p. 608–619.

[6] S. C. Tidwell, G. H. Kim, and W. D. Kimura, "Efficient radially polarized laser beam generation using a double-interferometer," Appl. Optics **32**, 5222-5229 (1993).

[7] L. V. Keldysh, "Ionization in the field of a strong electromagnetic wave, "Sov. Phys. JETP **20**, 1307 (1965).